

# Quantum control by ultrafast dressed states tailoring

M. Wollenhaupt, D. Liese, A. Präkelt, C. Sarpe-Tudoran, T. Baumert \*

*University of Kassel, Institute of Physics, Center for Interdisciplinary Nanostructure Science and Technology (CINSA-T),  
Heinrich-Plett-Strasse 40, D-34132 Kassel, Germany*

Received 10 November 2005

Available online 15 December 2005

## Abstract

Strong field quantum control using shaped intense femtosecond laser pulses is investigated. The physical mechanism relies on selective population of dressed states (SPODS). With time resolved photoelectron spectroscopy the ultrafast dressed state population dynamics during the ionization of potassium atoms is directly observed. High selectivity of the dressed state population and tunability of the dressed state energies is demonstrated experimentally. Wave packet simulations on a diatomic model molecule confirm that SPODS is also applicable to molecules. We conclude that SPODS with simple ultrashort optimal pulse shapes is suitable for robust laser control of chemical reactions.

© 2005 Elsevier B.V. All rights reserved.

## 1. Introduction

A central goal in physical chemistry is to control the outcome of a chemical reaction with light. With the advent of ultrashort femtosecond laser pulses the temporal aspect of the interplay of light and molecular dynamics came to the fore and became experimentally accessible. The beauty of femtochemistry – as the emerging field was termed by the 1999 Noble Prize winner Zewail [1] – lies in our ability to observe and to manipulate ultrafast processes as they occur. Shaped femtosecond optical laser pulses [2] are the suitable tools to exert microscopic control on molecular dynamics at the quantum level.

This technique has opened up new perspectives in research areas ranging from basic research to applications in physics, biology and chemistry. Numerous concepts for quantum control based on the quantum interference of matter waves have been devised which are summarized in recent monographs [3,4]. Generally, the underlying physical mechanisms are well understood for weak field quantum control schemes. In this weak field limit the population of the initial state – describing the system without the perturbation – is

constant during the interaction with the external light field. Strong laser fields, i.e. fields that are intense enough to effectively depopulate the initial state offer a rich variety of further mechanisms. Adiabatic strong field techniques such as rapid adiabatic passage or stimulated Raman adiabatic passage [4,5] are employed for instance with laser pulses in the picosecond to nanosecond domain allowing for population transfer with unit efficiency in quantum state systems. With the help of strong ultrashort laser pulses in the femtosecond domain the course of reactions has been modified after the initial excitation by altering the potential surfaces [6,7]. Recently, it was demonstrated that weak field quantum control concepts remain valid in strong amplitude modulated laser fields [8], i.e. fields with a constant instantaneous frequency. As a consequence, strong field techniques involving additional time varying phases such as phase jumps [9] or chirps [10] offer new prospects for quantum control and the clarification of hitherto not considered physical mechanisms.

In cases where the underlying potential surfaces are unknown an alternative approach based on a combination of pulse shaping techniques with adaptive feedback learning loops is used [11–16]. Implementations of this technique demonstrate the optimization of almost any conceivable physical quantity as highlighted in recent

\* Corresponding author. Fax: +49 561 804 4453.

E-mail address: [baumert@physik.uni-kassel.de](mailto:baumert@physik.uni-kassel.de) (T. Baumert).

reviews [17–19]. These so-called optimal control experiments are very general in the sense that they always deliver an optimal pulse for a given objective. However, the pulse shapes resulting from the optimization procedure are generally complicated and not uniquely defined. The complex topology of the parameter space involved in optimal control approaches was recently discussed in terms of quantum control landscapes theoretically [20] and experimentally [21]. The enormous success of optimal control strategies suggests the existence of robust strong field mechanisms being at play in these experiments. In order to unveil the physical mechanism, our experimental approach is based on the investigation of quantum control on a simple well defined model system (potassium atoms) excited by well characterized shaped intense laser pulses. Our strong field quantum control scheme – based on concepts originally developed in NMR (spin-locking) [22] – makes explicit use of temporal phase changes within the pulse and therefore weak field descriptions are no longer applicable [8]. The optical analogue of spin-locking termed photon-locking [23,24] was demonstrated experimentally using nano-second laser pulses [23,25]. We extend these techniques to the femtosecond time scale with relevant applications to femtochemistry. Generalizing these principles results in a physically comprehensible mechanism for strong field control with shaped femtosecond pulses based on selective population of dressed states (SPODS).

To that end we will first present an experimental implementation of SPODS on potassium atoms. In our experiment a single shaped intense pulse is used to induce the dynamics in the neutral atom and also to ionize the system. We measure kinetic energy resolved photoelectron spectra as a function of the pulse properties. We show how a high degree of selectivity of the dressed state population is obtained by control of the optical phase of our shaped laser pulses and how tunability of the dressed state energies in the several hundred meV range is achieved by control of the laser intensity. We then discuss our findings with respect to control of chemical reactions driven by multi photon schemes. Quantum control making use of SPODS is particularly attractive for applications to chemistry because it switches between different reaction pathways within a few femtoseconds. Finally, by wave packet simulations on a generic diatomic molecule, we confirm selectivity and tunability of SPODS in the presence of nuclear motion and ultrafast efficient population transfer to target states.

## 2. Experiment

The excitation and ionisation scheme of potassium atoms used in our experiment is depicted in Fig. 1a. The interaction of the 4s and 4p bare states (thin horizontal lines in Fig. 1a) with near resonant intense femtosecond radiation (785 nm, 30 fs) gives rise to the dressed states (bold lines), i.e. the eigenstates of the Hamiltonian which includes the laser matter interaction [26,27]. The latter

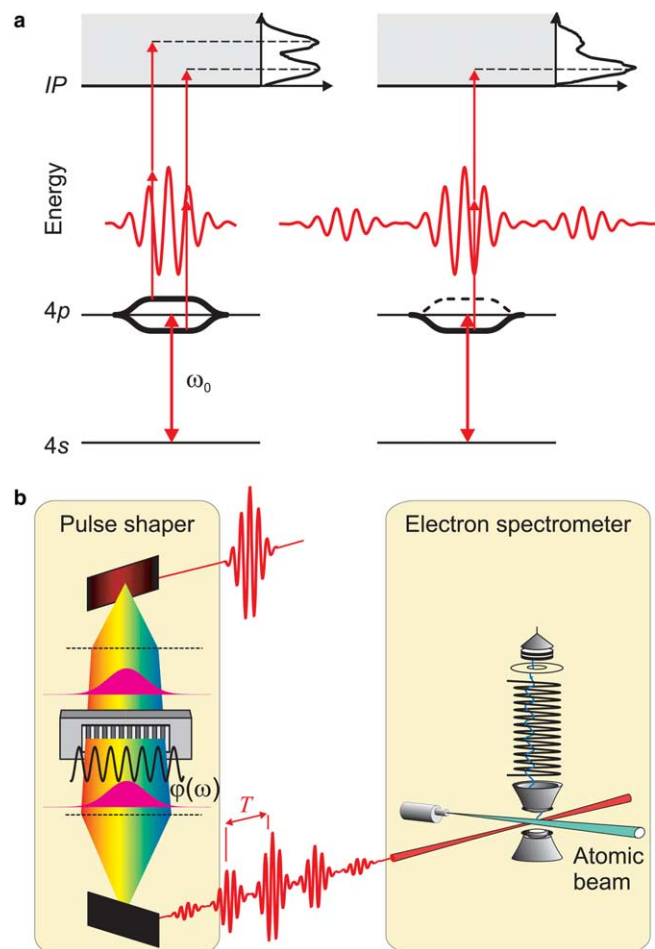


Fig. 1. Schematic of the excitation scheme for potassium atoms (a) and the experimental setup (b). For details see text.

are mapped into the photoelectron spectra during the light-matter interaction by two-photon ionisation similar to a one plus two resonant multi photon ionization process. Therefore, a natural physical interpretation of our results is given in terms of dressed states. As shown in Fig. 1a (left) excitation with unmodulated (or purely amplitude modulated) laser pulses leads to equal population of both dressed states [10] which gives rise to the symmetric splitting of the photoelectron spectrum – known as the Autler–Townes doublet. In view of chemical control, equal final states populations (i.e. symmetric photoelectron spectra) means no product selectivity. However, with suitable phase shaped pulses SPODS – and hence selectivity of the photo products – is achieved. For example, photo ionization from the (selectively populated) lower dressed state (Fig. 1a, right) produces exclusively low energy photoelectrons.

The experimental implementation of SPODS (Fig. 1b) is based on the combination of femtosecond pulse shaping techniques with atomic time-of-flight photoelectron spectroscopy. In our experimental setup (see Fig. 1b) the spectrum of a femtosecond laser pulse (785 nm, 30 fs, 0.35–2  $\mu$ J) is phase-modulated in frequency domain with our home-built pulse shaper [28] using a sinusoidal phase

function  $\varphi(\omega) = A \sin[(\omega - \omega_0)T + \phi]$  with  $A = 0.2$ ,  $T = 170$  fs and  $\omega_0 = 2.40$  fs $^{-1}$  to produce a sequence of pulses in time domain separated by  $T$ . These pulses are focussed with a lens ( $f = 300$  mm) into a vacuum chamber to interact with potassium atoms. Kinetic electrons from the simultaneous excitation and photo ionization are detected via a magnetic bottle photoelectron spectrometer as a function of  $\phi$  ( $\phi$  determines the phase of the individual sub-pulses). Sinusoidal phase modulation is a convenient parameterization for complex pulse shapes and is often used in current quantum control experiments [29–32]. This modulation produces a sequence of pulses separated by the delay  $T$ . The amplitude of these sub-pulses is determined by the amplitude  $A$  and the relative optical phase of these sub-pulses is controlled by the parameter  $\phi$  (see for example [32]). No interferometric phase stabilization is needed in this approach. A representative modulated electrical field is depicted in Fig. 1b. It consists of five sub-pulses. Focussing these pulses onto potassium atoms in the beam results in a specific excitation and ionization sequence that will be shortly summarized here whereas a detailed discussion is

given later. The first sub-pulse is weak enough to introduce only a small perturbation. The second sub-pulse with a pulse area of  $\pi/2$  creates a coherent superposition of both  $4s$  and  $4p$  states. The third and most intense sub-pulse probes this coherence by two photon ionization. Although ionization occurs during all sub-pulses, the observed photoelectron spectrum predominantly maps the dressed state population during this most intense sub-pulse.

### 3. Results and discussion

Typical experimental results obtained at a pulse energy of  $0.5$   $\mu\text{J}$  are displayed in Fig. 2 (3-D graph). By variation of  $\phi$  the maximum in the photoelectron distribution alternates between low ( $0.33$  eV) and high ( $0.52$  eV) kinetic energies. These measured photoelectron spectra are strongly asymmetric. Sections through the data along the kinetic energy axis, as indicated with the violet and magenta trajectories on the 3-D graph, yield photoelectron spectra at a particular value of  $\phi$ . For instance, the section at  $\phi = 0.7\pi$  – indicated with the violet trajectory – yields

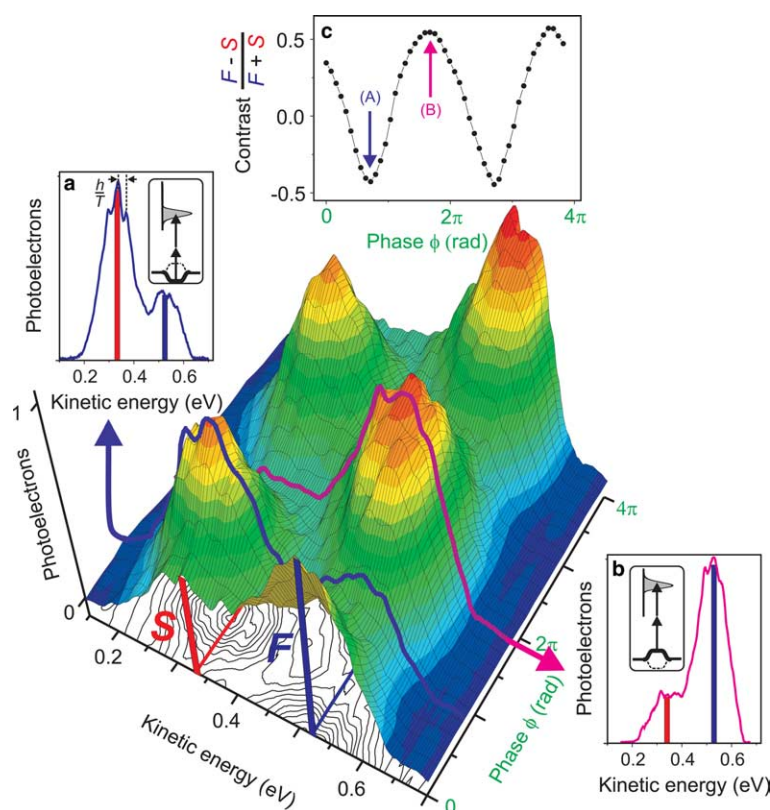


Fig. 2. The selective population of dressed states (SPODS) is directly mapped into the measured photoelectron spectra by variation of the phase  $\phi$ . These results are obtained at a laser energy of  $W = 0.5$   $\mu\text{J}$ . A section through the distribution along the energy axis at  $\phi = 0.7\pi$  – indicated with the violet trajectory – yields the photoelectron spectrum (a) where the lower dressed state is selectively populated as depicted in the inset to (a). Fringes in the spectrum with an energy separation of  $h/T$  arise from the interference of the free electron wave packets launched during the different pulses. Selective population of the upper dressed state is achieved at  $\phi = 1.7\pi$  as indicated with the magenta trajectory and plotted in spectrum (b). The signal of the slow photoelectrons at  $0.33$  eV ( $S$ ) and the fast photoelectrons at  $0.52$  eV ( $F$ ) – as indicated with the red and blue bars – is obtained as a function of the phase  $\phi$  by taking a section through the distribution along the phase coordinate. The contrast of  $F$  and  $S$ , i.e.  $(F - S)/(F + S)$  as shown in (c) is a measure of the selectivity of dressed state population. The phases corresponding to the highest selectivity for population of the lower dressed state – spectrum (a) – and the upper dressed state – spectrum (b) – are indicated with violet and magenta arrows, respectively.

the photoelectron spectrum displayed in Fig. 2a. This spectrum is dominated by a photoelectron peak at low kinetic energies (0.33 eV) corresponding to selective population of the lower dressed state as shown schematically in the inset to Fig. 2a. In contrast, the spectrum at  $\phi = 1.7\pi$  (Fig. 2b) predominantly shows fast photoelectrons at 0.52 eV. Here the upper dressed state is populated selectively. In order to quantitatively evaluate the selectivity we consider the signal of slow photoelectrons at 0.33 eV ( $S$ ) and fast photoelectrons at 0.52 eV ( $F$ ) indicated with red and blue bars in the 3-D graph and in both spectra (Fig. 2a,b). The contrast of both values is shown in Fig. 2c. It is defined as  $(F - S)/(F + S)$  and characterizes the asymmetry of the photoelectron spectra. This contrast is a measure of the selectivity. The contrast ranges from  $-0.45$  (violet arrow in (c) corresponding to the spectrum in Fig. 2a) to  $+0.56$  (magenta arrow in (c) corresponding to the spectrum in Fig. 2b). Note that a contrast of  $+0.56$  is equivalent to almost 80% population in the upper dressed state. The strong modulation of the contrast (Fig. 2c) demonstrates the high degree of selectivity attained in our experiment and our ability to switch between selective population of both upper and lower dressed states with high efficiency. Recently we employed adaptive pulse shaping techniques and achieved up to 90% selective population of a single dressed state [33]. The  $2\pi$ -periodicity of the contrast originates from the  $2\pi$ -periodicity of the sine phase function. In addition, reproducible interference fringes are observed in the spectra. They arise from the interference of free electron wave packets launched during different sub-pulses. Their energy separation of  $h/T$  is indicated in Fig. 2a. Such interferences are reminiscent of the Young's double slit experiment performed in time rather than in space. Experimental realizations of the temporal double slit were reported using either weak [34] or strong [33] femtosecond pulse sequences and more recently attosecond pulses [35].

Although we use a multi-pulse sequence for convenience (see above) the essential physical mechanism for the selectivity of SPODS is based on a two step process. First the  $\pi/2$  (pulse area) sub-pulse creates a coherent superposition with both 4s and 4p states equally populated. Then, the relative phase between this sub-pulse and the subsequent (most intense) sub-pulse – determined by  $\phi$  – controls the dressed state population during the most intense sub-pulse. If the relative phase is 0 or  $\pi$  both dressed states are equally populated and mapped into a symmetric photoelectron spectrum. If the relative phase is  $\pm\pi/2$  the bare state population is frozen (photon locking) during the interaction with the most intense sub-pulse corresponding to selective population of the upper or the lower dressed state as observed by the asymmetric spectrum. Switching between selective population of either dressed states occurs within an optical cycle. Accordingly, adiabatic conditions are not required during the complete process.

So far we exerted phase control to select a single dressed state at a given energy separation  $\hbar\Omega$  between both dressed

states where  $\Omega$  denotes the Rabi frequency. In view of applications to quantum control, selectivity and efficient population transfer to specific target states are both important. The latter is achieved by tuning the dressed state energies into resonance with the (also dressed) target states. In this section we present our experimental results on the tunability of the dressed state energies by variation of the laser intensity. Since the energy splitting  $\hbar\Omega = \mu\varepsilon$  is proportional to the dipole moment  $\mu$  times the laser electrical field  $\varepsilon$  – which in turn is proportional to the square root of the laser pulse intensity ( $I(\varepsilon \propto I^{0.5})$ ) – we use the pulse energy  $W$  – which is proportional to the intensity for a given pulse duration  $\Delta t$  and a given laser spot size – as a convenient experimental parameter to tune the energy of the dressed states. From these considerations we expect a square root dependence of the measured energy splitting  $\hbar\Omega \propto I^{0.5}$  with respect to the pulse energy.

The results for laser energies ranging from 0.35 to 2  $\mu\text{J}$  are shown in a logarithmic representation (Fig. 3). In order to determine the energy splitting of the photoelectron spectra the sum of two Gaussians was fitted to the measured spectra. The centres of both Gaussians are plotted as open circles on top of the spectra. The increase of the splitting with increasing laser pulse energy is visualized with red and blue dashed lines. The splitting of  $\hbar\Omega = 150$  meV at the lowest laser energy (0.35  $\mu\text{J}$ ) and  $\hbar\Omega = 270$  meV at the highest laser energy (2  $\mu\text{J}$ ) of our measurements is indicated with black bars. For comparison, the spectral width of a 30 fs laser pulse ( $\hbar\Delta\omega = 60$  meV) is also shown. In fact, the tunability achieved by strong field control exceeds the laser bandwidth by a factor of 4.5. The inset to Fig. 3 shows a log–log plot of the energetic splitting  $\hbar\Omega$  as a function of the laser pulse energy  $W$ . The observed energy

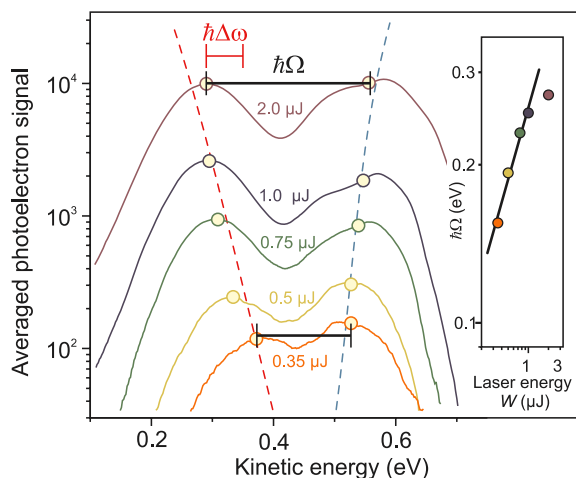


Fig. 3. The energy tunability of the dressed states is demonstrated on the splitting  $\hbar\Omega$  of the photoelectron spectra as a function of laser energy  $W$ . For the lowest laser energy and the highest laser energy the splitting  $\hbar\Omega$  is 150 and 270 meV, respectively (black bars). The spectral width  $\hbar\Delta\omega$  of a 30 fs laser pulse (60 meV) is shown for comparison. Dotted lines indicate the trend of the splitting with increasing laser energy. The inset shows a log–log plot of  $\hbar\Omega$  as a function of the pulse energy  $W$ . The observed slope of  $0.46 \pm 0.04$  confirms that the splitting increases with the square root of the laser intensity ( $\hbar\Omega \propto I^{0.5}$ ).

dependence  $\hbar\Omega \propto W^{0.46 \pm 0.04}$  confirms the expected square root dependence. At energies around  $2 \mu\text{J}$  the curve starts to saturate because higher excited states of the potassium atom take part in the excitation process.

#### 4. Control of chemical reactions

We now turn to the discussion of our experimental findings with respect to the control of photochemical reactions. In order to explore the validity of the proposed strong field mechanism in the presence of further degrees of freedom such as vibrations we simulate the corresponding wave packet dynamics on a generic diatomic model molecule. The potentials of this molecule are shown in Fig. 4a. At the vibrational equilibrium position, the electronic ground state X and the first excited state A are in resonance with the laser radiation. These states are coupled by a dipole moment  $\mu_0$  whereas the coupling to the non-resonant higher excited states (B ← A and C ← A) is described by  $0.3 \mu_0$ . These dipole moments are similar to those of resonant excitation sequences in alkali dimers. The detuning of the excited state transitions at the equilibrium position with respect to the laser wavelength is in the order of  $\pm 150 \text{ meV}$ . To analyze the validity of the two step physical process outlined above, the wave packet dynamics is controlled by a simple shaped pulse (bold line in Fig. 4d shows the envelope of the pulse) with a rapid change of phase (dashed line in Fig. 4d). The pulse duration is short in comparison to half a vibrational period. In order to exert additional control during the course of the reaction, other potentially more complex pulse shapes can be designed. The simulations are performed by iteratively

solving the time dependent Schrödinger equation for the light induced dynamics on all four potentials using a grid based representation of the wave function propagated in time by a Fourier based split-operator method (see for example [4]).

We analyze the excitation process with respect to the time dependent population of each state (Fig. 4c). Initially the molecule is in the vibronic ground state (Fig. 4a). The first part of the pulse excites about 50% of the ground state population into the A state creating a coherent superposition of the X and the A states (cf. dotted vertical line at around 10 fs in the plot of the population traces in Fig. 4b). During the trailing edge of the pulse, the resonance enhanced two-photon excitation of the B and C states via the A state is suppressed due to their detuning of about 150 meV. As a consequence both states are negligibly populated at around 10 fs (cf. population of the B and C states at around 10 fs in Fig. 4c). The A state wave packet has not moved markedly when the intense part of the pulse arrives at the molecule. During this part of the pulse the optical phase is approximately  $-\pi/2$ . Thus photon locking of the resonant X and A states is realized. The system remains in the maximum coherent state while no significant population transfer, i.e. Rabi oscillations, occurs between the X and A states. In the dressed state picture, this uncommon dynamics corresponds to selective population of a single dressed state as depicted in Fig. 4b. As in the atomic case, the phase jump controls which of the dressed states is selectively populated. In particular, a phase jump of approximately  $-\pi/2$  leads to selective population of the lower dressed state ( $A_{\text{low}}$ ) as indicated with the bold line in Fig. 4b. The intensity of the pulse during SPODS was adjusted to shift  $A_{\text{low}}$  into res-

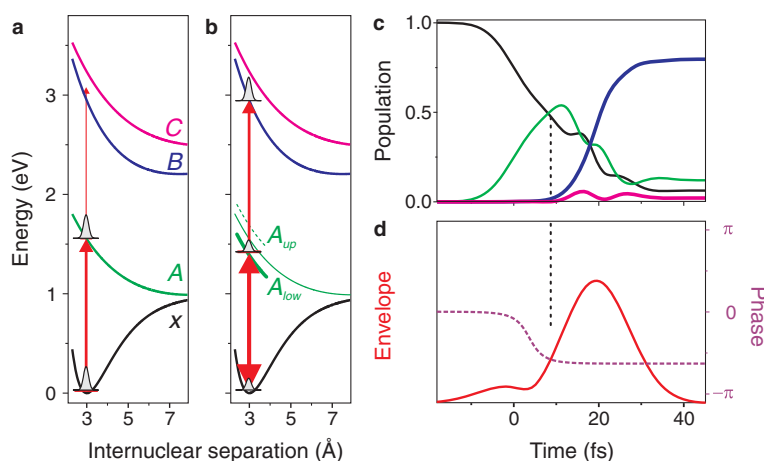


Fig. 4. Wave packet simulation of SPODS for a model molecule. Potential scheme for the excitation during the first part of the pulse (a) and the second part of the pulse (b). The time evolution of the population of the states X (black), A (green), B (blue) and C (magenta) is shown in (c). The envelope (red) and phase (dotted violet) of the laser electric field is plotted in (d). After the first part of the pulse, 50% of the ground state population is pumped from the X to the A state – cf. panel (a) and the vertical dotted line at about 10 fs in panel (c). Further excitation to the B and C states is suppressed (cf. low population in the B and C states at about 10 fs) because both states are off-resonant by 150 meV. Because the optical phase of the second part of the pulse jumps about  $-\pi/2$  only the lower dressed state  $A_{\text{low}}$  is selectively populated during the interaction with the most intense part of the pulse as shown in panel (b). During this period, the B state is resonant with the lower dressed state ( $A_{\text{low}}$ ) and therefore population is pumped into the B state with high efficiency as seen in (c).

onance with the B state. As a consequence, during this pulse, the population is selectively transferred to the B state with high efficiency. Indeed, after the pulse, 80% of the population is stored in the B state whereas only 2% arrives in the C state similar to our experimental findings on atoms. On the first glance it seems surprising that SPODS prevails despite the significant loss of population in both the X and the A states. However, for SPODS to proceed, the phase ( $\pm\pi/2$ ) of the intense part of the pulse and the coherence properties of the photon locked states are crucial rather than their absolute population. Setting the optical phase to approximately  $+\pi/2$  during the intense part of the pulse reverses the picture (not shown in Fig. 4). In this case the upper dressed state ( $A_{\text{up}}$ ) is selectively populated and shifted by  $\hbar\Omega/2$  into resonance with the C state. As a consequence the C state is populated efficiently at the expense of the B state population. Our simulations on this generic molecular model system show, that the strong field physical mechanism based on SPODS is also applicable to molecules. Further simulations show that the mechanism is robust with respect to the pulse parameters. In addition, we believe that SPODS will be generally applicable since the mechanism does not depend on the details of the potential energy surface.

## 5. Summary

In summary, we demonstrate a strong field multi photon quantum control scenario based on ultrafast dressed states tailoring with potential applications to laser control of chemical reactions. In the experiment, shaped intense femtosecond laser pulses are used to control the electronic dynamics of potassium atoms. We use sinusoidal phase modulation in frequency domain as a convenient way to generate pulse sequences in time domain with well defined relative phases and amplitudes of the individual sub-pulses. By that we reduce the physical mechanism induced by a shaped pulse to a two step process induced by a ‘weak’  $\pi/2$  (pulse area) preparation sub-pulse followed by a ‘strong’ sub-pulse. The relative phase between these sub-pulses controls the population of dressed states whereas the intensity of the ‘strong’ pulse controls the dressed state splitting. This dynamical information is obtained by observation of photoelectron spectra. The insights into the physical mechanism of dressed state tailoring permits us to design specific tailored strong field pulse shapes in order to maximize the laser control efficiency in other circumstances as well. In order to validate SPODS in molecules possessing further degrees of freedom we perform wave packet studies on a generic diatomic molecule. On this model system, we show how phase discontinuities within suitably shaped pulses act as an ultrafast switch among different reaction channels. This switch can also be operated during the course of a reaction. In addition our simulations confirm that SPODS is applicable to molecules in the presence of non-perturbative population transfer to the

target states. Similar to our experimental results on atoms, our simulations on molecules show that SPODS combines high selectivity and tunability with efficient population transfer. Experimental demonstrations of SPODS on molecules are currently prepared in our labs.

## Acknowledgements

The authors thank G. Gerber, Y. Silberberg and A.H. Zewail for their helpful comments on the manuscript. The financial support by the Deutsche Forschungsgemeinschaft is gratefully acknowledged.

## References

- [1] A.H. Zewail, *J. Phys. Chem.* 104 (2000) 5660.
- [2] A.M. Weiner, *Rev. Sci. Instrum.* 71 (2000) 1929.
- [3] M. Shapiro, P. Brumer, *Principles of the Quantum Control of Molecular Processes*, first edn., Wiley, Hoboken, NJ, 2003.
- [4] S.A. Rice, M. Zhao, *Optical Control of Molecular Dynamics*, Wiley, New York, 2000.
- [5] N.V. Vitanov, T. Halfmann, B.W. Shore, K. Bergmann, *Annu. Rev. Phys. Chem.* 52 (2001) 763.
- [6] T. Frohnmeyer, M. Hofmann, M. Strehle, T. Baumert, *Chem. Phys. Lett.* 312 (1999) 447.
- [7] J.G. Underwood, M. Spanner, M.Y. Ivanov, J. Mottershead, B.J. Sussman, A. Stolow, *Phys. Rev. Lett.* 90 (2003) 223001-1.
- [8] N. Dudovich, T. Polack, A. Pe'er, Y. Silberberg, *Phys. Rev. Lett.* 94 (2005) 083002-1.
- [9] M. Wollenhaupt, A. Assion, O. Bazhan, C. Horn, D. Liese, C. Sarpe-Tudoran, M. Winter, T. Baumert, *Phys. Rev. A* 68 (2003) 015401-1.
- [10] M. Wollenhaupt, A. Präkelt, C. Sarpe-Tudoran, D. Liese, T. Baumert, *Appl. Phys. B* (in print).
- [11] R.S. Judson, H. Rabitz, *Phys. Rev. Lett.* 68 (1992) 1500.
- [12] T. Baumert, T. Brixner, V. Seyfried, M. Strehle, G. Gerber, *Appl. Phys. B* 65 (1997) 779.
- [13] C.J. Bardeen, V.V. Yakolev, K.R. Wilson, S.D. Carpenter, P.M. Weber, W.S. Warren, *Chem. Phys. Lett.* 280 (1997) 151.
- [14] D. Yelin, D. Meshulach, Y. Silberberg, *Opt. Lett.* 22 (1997) 1793.
- [15] A. Assion, T. Baumert, M. Bergt, T. Brixner, B. Kiefer, V. Seyfried, M. Strehle, G. Gerber, *Science* 282 (1998) 919.
- [16] R.J. Levis, G.M. Menkir, H. Rabitz, *Science* 292 (2001) 709.
- [17] T. Brixner, T. Pfeifer, G. Gerber, M. Wollenhaupt, T. Baumert, in: P. Hannaford (Ed.), *Femtosecond Laser Spectroscopy*, Kluwer Series, 2004, pp. 225–266 (Chapter 9).
- [18] D. Goswami, *Phys. Rep.* 374 (2003) 385.
- [19] M. Dantus, V.V. Lozovoy, *Chem. Rev.* 104 (2004) 1813.
- [20] H.A. Rabitz, M.M. Hsieh, C.M. Rosenthal, *Science* 303 (2004) 1998.
- [21] M. Wollenhaupt, A. Präkelt, C. Sarpe-Tudoran, D. Liese, T. Baumert, *J. Mod. Opt.* 52 (2005) 2187.
- [22] S.R. Hartmann, E.L. Hahn, *Phys. Rev.* 128 (1962) 2053.
- [23] E.T. Sleva, I.M. Xavier Jr., A.H. Zewail, *JOSA B* 3 (1985) 483.
- [24] R. Kosloff, A.D. Hammerich, D. Tannor, *Phys. Rev. Lett.* 69 (1992) 2172.
- [25] Y.S. Bai, A.G. Yodh, T.W. Mossberg, *Phys. Rev. Lett.* 55 (1985) 1277.
- [26] B.W. Shore *The Theory of Coherent Atomic Excitation*, vol. 1, Wiley, New York, 1990.
- [27] M. Wollenhaupt, V. Engel, T. Baumert, *Annu. Rev. Phys. Chem.* 56 (2005) 25.
- [28] A. Präkelt, M. Wollenhaupt, A. Assion, C. Horn, C. Sarpe-Tudoran, M. Winter, T. Baumert, *Rev. Sci. Instrum.* 74 (2003) 4950.
- [29] D. Meshulach, Y. Silberberg, *Nature* 396 (1998) 239.
- [30] J.L. Herek, W. Wohlleben, R. Cogdell, D. Zeidler, M. Motzkus, *Nature* 417 (2002) 533.

- [31] A. Bartelt, A. Lindinger, C. Lupulescu, S. Vajda, L. Wöste, *Phys. Chem. Chem. Phys.* 5 (2003) 3610.
- [32] A. Präkelt, M. Wollenhaupt, C. Sarpe-Tudoran, T. Baumert, *Phys. Rev. A* 70 (2004) 063407-1.
- [33] M. Wollenhaupt, A. Präkelt, C. Sarpe-Tudoran, D. Liese, T. Baumert, *J. Opt. B* 7 (2005) S270.
- [34] M. Wollenhaupt, A. Assion, D. Liese, C. Sarpe-Tudoran, T. Baumert, S. Zamith, M.A. Bouchene, B. Girard, A. Flettner, U. Weichmann, G. Gerber, *Phys. Rev. Lett.* 89 (2002) 173001-1.
- [35] F. Lindner, M.G. Schätzel, H. Walther, A. Baltuska, E. Goulielmakis, F. Krausz, D.B. Milosevic, D. Bauer, W. Becker, G.G. Paulus, *Phys. Rev. Lett.* 95 (2005) 040401-1.